AmericaView
Mini-Grant Opportunity
Grant Year 2015

Project Title: Quantifying change in riparian vegetation in the Genesee River and exploring relationship to seasonal weather patterns and downstream water quality

Authors: Dr. Lindi J. Quackenbush (ljquack@esf.edu), Associate Professor, NYView PI
Ge Pu (gpu100@syr.edu), PhD Student

Institution: State University of New York College of Environmental Science and Forestry
1 Forestry Drive, Syracuse NY 13210

Project period: 16 October 2016 – 31 December 2016

Introduction

Riparian areas form the boundaries between terrestrial and aquatic ecosystems and provide critical functions in hydrology, geomorphology and biology (Brinson et al. 2002). Vegetation within riparian areas, also known as riparian buffers, plays a key role in providing these functions through decreasing flow of runoff and floodwater, creating soil macrospores through root growth and decay, stabilizing streambanks through root systems, and filtering contamination and maintaining stream water quality (NYSDEC Great Lakes Watershed Program 2014). Recent studies have also suggested small differences in riparian vegetation cover can significantly reduce run-off related effects of agriculture (Chase et al. 2016).

When natural riparian areas are altered by humans, such as through agricultural practices or channelization, these areas are no longer capable of providing their important ecological functions. Jones et al. (2010) reported that the total amount of forest and natural land cover in riparian areas declined in the majority of the continental US from 1972 to 2003. Since then, major effort has been invested in evaluating these areas. Yet, we still lack comprehensive maps of the location and condition of riparian areas (Salo and Theobald 2016). Moreover, there is no reliable and feasible method to regularly evaluate and monitor trends in riparian areas.

New methodologies should take advantage of recent technological advances in remote sensing, geographic information systems, Big Data and cloud computing (e.g. Google Earth Engine) to better address the current issues, and to better aid riparian restoration efforts on the ground. This project focused on developing a method to enable multi-temporal assessment of riparian vegetation extent and condition, as well taking a step toward linking remotely sensed riparian vegetation data with downstream water quality parameters and local weather patterns.

Methodology

Study Area. This study focused on the main stem of the Genesee River, which originates in Gold, PA and flows north to Rochester, NY with a total length of 247 km and a 6407.6 km^2 watershed area. Land cover in the area is dominated by agriculture (52%) and forest (40%), with smaller amounts of developed land (4.6%), including a mixture of residential, commercial, industrial, and transportation/utilities uses, wetlands and water (2%), and other non-developed lands (1.4%) (Makarewicz et al. 2015). Various parts of the Genesee River are currently listed as impaired on Section 303 (d) of the Federal Clean Water Act based on the presence of various pollutants, which includes phosphorus, sedimentation, oxygen demand, and pathogens (NYSDEC 2014). This watershed is of particular importance because the Genesee River discharges into Lake Ontario, a part of the largest body of freshwater in the world, the Great Lakes. Under these circumstances, riparian buffers along the Genesee River play a significant role in improving the overall condition of the river and help combat many of the water quality related problems through filtering various contaminations, trapping sedimentation and ultimately improving river water quality.

The Mount Morris gravity dam (42.731° N, 77.904° W) on the Genesee River (Figure 1) was utilized as a separation point when comparing the results of riparian vegetation indices. This separation formed a logical break since upstream of the dam the channel follows its natural path, whereas flow downstream of the dam is regulated by the dam instead of natural flow regimes.

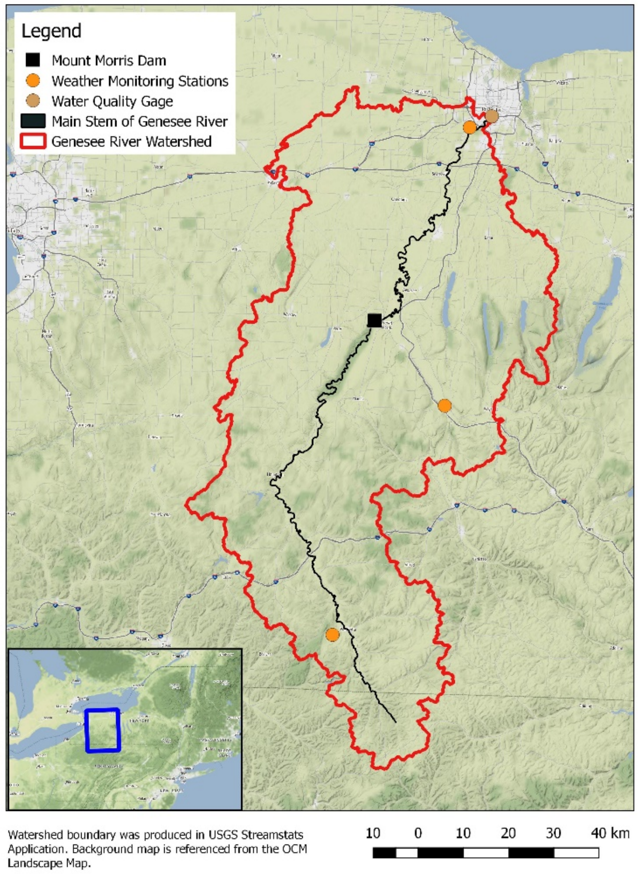

Figure 1. Map of Genesee River watershed boundary

Data. Remotely sensed datasets utilized in this study focused on two freely accessible image programs: (1) United States Department of Agriculture National Agriculture Imagery Program (NAIP) imagery, and (2) Landsat products. Both datasets are available through Google Earth Engine (GEE). The NAIP images are airborne color-infrared orthorectified images acquired at 1 meter ground sampling distance. This fine spatial resolution enables interpolation of detailed information on the boundaries of river channels and riparian vegetation. The NAIP program collects imagery on a regular basis, with images of the study area available from 2003–2015. GEE provides access to Landsat 5 and 8 8-day Normalized Difference Vegetation Index (NDVI) and Enhanced Vegetation Index (EVI) composites (https://code.earthengine.google.com/). These data were provided by Google through compiling Landsat 5 and 8 L1T orthorectified scenes. On an 8-day basis, this compilation provides NDVI and EVI values for each pixel within the image. Computation of NDVI and EVI values were generated through Equation 1 and Equation 2, respectively, shown below:

$$\mathbf{NDVI} = \frac{\mathbf{NIR - RED}}{\mathbf{NIR + RED}} \qquad \textbf{Equation 1}$$

Where NIR and RED are atmospherically-corrected or partially corrected surface reflectance from the near infrared and red portions of the spectrum, respectively.

$$\mathbf{EVI} = \mathbf{G} \times \frac{\mathbf{NIR - RED}}{\mathbf{NIR + C_1 \times RED - C_2 \times BLUE + L}} \qquad \textbf{Equation 2}$$

Where BLUE is atmospherically-corrected or partially corrected surface reflectance from the blue portion of the spectrum, L is the canopy background adjustment that addresses non-linear, differential NIR and red radiant transfer through a canopy, C1 and C2 are the coefficients of the aerosol resistance term, which uses the blue band to correct for aerosol influences in the red band, and G is the grain factor (USGS 2016). L, C1, C2, and G values are referenced from the study published by Huete et al. (2002). The vegetation index datasets were critical in assessing the historical trends in riparian vegetation vigor. Data availability is 1984–2012 for Landsat 5 composites, and from 2013–2016 for Landsat 8 composites.

Two publicly accessible in-situ datasets were also utilized in this study: (1) United States Geological Survey (USGS) water quality data, and (2) National Oceanic and Atmospheric Administration (NOAA) weather data. Downstream water quality data was collected by the USGS in the Genesee River at the Ford Street Bridge in Rochester, NY and downloaded through the USGS Water Data for the Nation website (https://waterdata.usgs.gov/usa/nwis/uv?04231600). Parameters collected include water temperature, specific conductivity, pH, turbidity and dissolved oxygen. Data is available at the site starting from 2010 and is recorded as daily maximum, minimum, and mean values. The study also used weather data collected by NOAA at three airports within the watershed: Greater Rochester International Airport, Cattaraugus County Olean Airport, and Dansville Municipal Airport (https://gis.ncdc.noaa.gov/maps/ncei/cdo/daily). These three stations were selected because their locations are distributed throughout the Genesee River watershed (Figure 1). Weather parameters recorded include daily mean precipitation and daily cumulative air temperature. Weather parameters across the three stations were averaged to eliminate micro climate effects. Available data varies by station, but data is available for all stations from 2004.

Study Duration. Comparing availability across all of the datasets utilized in this study, the duration of the study considering the relationship between water parameters and riparian buffer extent was limited to 2010–2015 based on the water quality data, which has the shortest availability. Exploration of the change in the stream channel, which did not use the water quality data, worked with imagery from 2006–2015. In both cases, there is a data gap in 2012 during the transition from Landsat 5 to Landsat 8 datasets.

Extracting Time Series of Riparian Vegetation Indices. This project developed a new method to extract multi-temporal riparian vegetation indices directly from satellite image composites. As shown in Figure 2, this process involved five major steps: (1) Identifying the channel boundary, (2) creating a buffer around the channel, (3) classifying land cover within the riparian buffer, (4) converting pixel-based vegetation buffers to polygons, and (5) generating final riparian buffer boundaries.

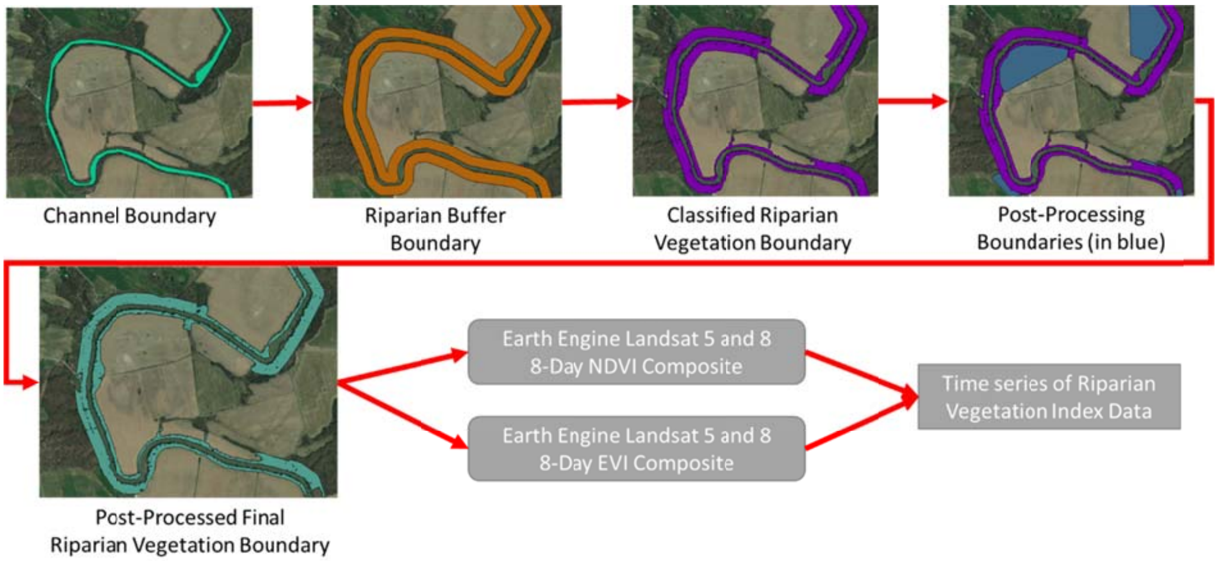

Figure 2. Process for extracting riparian vegetation index time series data.

The first stage of the process involved manually delineating channel boundaries of the main stem of the river in GEE using the USDA NAIP imagery. Since NAIP images were available for the study site in alternating years and the location of the channel demonstrated annual variability, separate channel boundaries were digitized separately for each NAIP image. Comparison of river stages on the days when the NAIP images were collected confirmed that the river stages were similar when the imagery were acquired. This reduced the possibility of mistakes in drawing channel boundaries due to extreme high and low river stages or differences in the channel boundaries due to variations in the river water depth during delineation. Having identified the main channel, the second stage of the process buffered each channel boundary to 90 m to create the limit of the riparian buffers. The selection of a 90 m buffer was based on work presented by Sweeney and Newbold (2014) who suggested 90 m riparian buffers are optimal to achieve the highest possible sediment removal efficiency.

The third step of the process was classifying the riparian buffer pixels as vegetation or non-vegetation. For each available year, the NAIP images were clipped using the riparian buffer boundaries and then the buffer zone was classified into vegetation and non-vegetation classes. Classifications utilized the random forest method (Pal 2005) using reference points that were randomly selected within the riparian buffer boundaries and visually assigned to vegetation or non-vegetation classes. The total number of reference samples for both above and below dam sections was 900. The distribution of points between vegetation and non-vegetation categories varied from image to image (Table 1).

Table 1. Distribution of reference points.

Year	Above dam		Below dam	
	Vegetation	Non-Vegetation	Vegetation	Non-Vegetation
2011	587	313	569	331
2013	649	251	712	649
2015	387	413	483	317

The inputs to the random forest classification included the reflectance for pixels within each NAIP image bands and the NDVI values derived from these bands. Half of the reference points were randomly selected and utilized in the classifier while the other half were utilized in accuracy verification through generating confusion matrixes. Optimization of the number of trees for the random forest classifier was performed in R, while buffering, clipping and classification of the images were done in GEE.

The classified images from the third step were then converted into vector polygons that delineated the boundaries of the vegetation within the buffered riparian area. These boundaries were then post-processed through manual identification to interpolate and remove agriculture vegetation. The decision to exclude agriculture vegetation was because this cover type does not provide key benefits such as filtering pollutants and trapping sedimentation, and agriculture is in fact the largest pollution source for phosphorus in the Genesee River (NYS DEC 2015). Upon cropping the agriculture vegetation, post processed final riparian vegetation boundaries were generated. Mean NDVI and EVI values derived from Landsat images across the entire boundaries were then extracted for each polygon on an 8-day basis. Since the NAIP imagery was not available each year, the post-processed riparian vegetation boundary derived from an available NAIP image was used to derive vegetation indices for that year and the following year e.g. the 2011 boundary was utilized to derive 2011 and 2012 vegetation indices. Finally, time series of mean NDVI and EVI from the Landsat data within the derived riparian vegetation boundaries were generated for the sections of the river above and below the dam.

Data Correlation. Correlation between daily water quality data, multi-temporal riparian vegetation indices, and weather data were evaluated using Spearman's correlation coefficient. This method was selected because the distribution of each dataset is likely not normal, especially for the water quality parameters.

Advantages of Utilizing Google Earth Engine. This project utilized GEE for both image processing and spatial analysis processes, along with some usage of QGIS (QGIS Development Team 2016). GEE is an online platform that incorporates data from various agencies, which includes full image collections from USDA NAIP program and the entire Landsat archive to date (Patel et al. 2014). GEE provides an efficient means to perform environmental data monitoring because it eliminates the processing time and effort involved with downloading, sorting, and combining datasets in order to perform the calculations and other processes necessary to obtain time series vegetation index data. Another benefit of GEE is easy scalability, with data and capacity to enable it to be utilized virtually globally. The script that was written in GEE for this project can be easily modified to be rapidly deployed in other regions in order to more broadly monitor and evaluate riparian vegetation extent and vigor.

Results and Discussion

Classification

Assessment of the classification of riparian vegetation vs. non-riparian vegetation using the validation data produced the confusion matrixes shown in
Table 3. Confusion Matrix for section of watershed below the dam. and Table 3.

Table 2. Confusion matrix for section of watershed above the dam.

Year	Producer		User		Overall Accuracy
	Vegetation	Non-vegetation	Vegetation	Non-vegetation	
2011	0.98	0.97	0.99	0.95	0.98
2013	0.98	0.96	0.98	0.94	0.97
2015	0.97	0.98	0.98	0.98	0.98

Table 3. Confusion Matrix for section of watershed below the dam.

Year	Producer		User		Overall Accuracy
	Vegetation	Non-vegetation	Vegetation	Non-vegetation	
2011	0.99	0.87	0.93	0.98	0.95
2013	0.99	0.95	0.99	0.96	0.98
2015	0.97	0.95	0.96	0.95	0.96

Overall and class accuracies were above 90% except for the non-vegetation producer's accuracy (87%) for the region below the dam in the 2011 imagery. These high accuracy values suggest that the initial classifications were successful. Note that these accuracies were calculated prior to performing the post-processing. While it is unlikely that the accuracy values would decrease due to post-processing, it is possible that the post-processing may increase the final accuracies of the riparian vegetation delineation.

Vegetation extent

Vegetation extent data derived from the NAIP imagery (Figure 3) show 10–20% fluctuations in vegetation coverage within the buffer from 2011–2015. The extent of vegetation cover within the 90m riparian buffer zone averages around 70% along the entire main stem of the Genesee River within this period. An exploration of the changes in extent, particularly in 2011 and 2015, suggest that the changes appear to be caused by shadows in the NAIP imagery. The inconsistency in the time of when the images were taken caused the classification to treat vegetation covered by shadows to be non-vegetation.

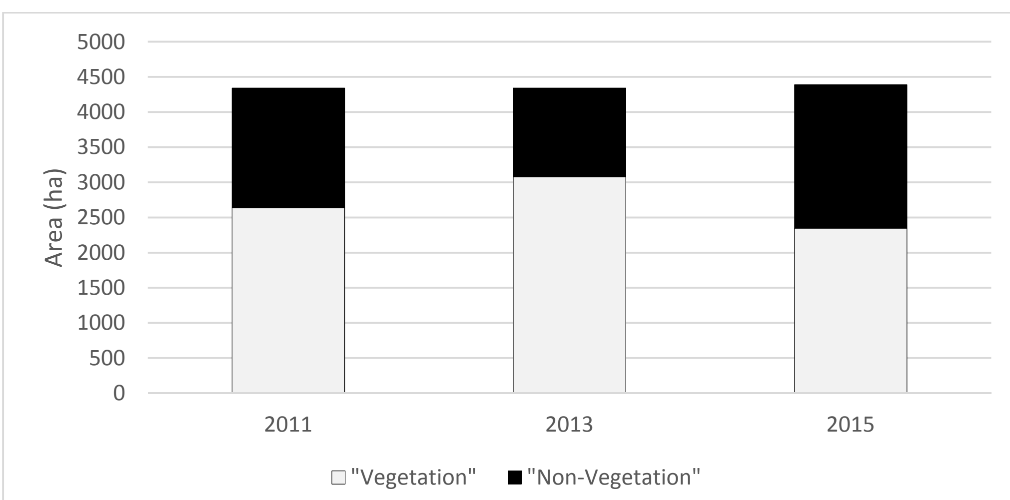

Figure 3. Temporal changes in buffered channel area and riparian vegetation extent.

An alternate approach to mapping the vegetation extent is to use the vegetation index data derived from the Landsat imagery. Figure 4 shows the 8-day composite and monthly time series plots of the values of the mean vegetation index within the riparian buffers calculated using the Landsat 5/8 8-day products.

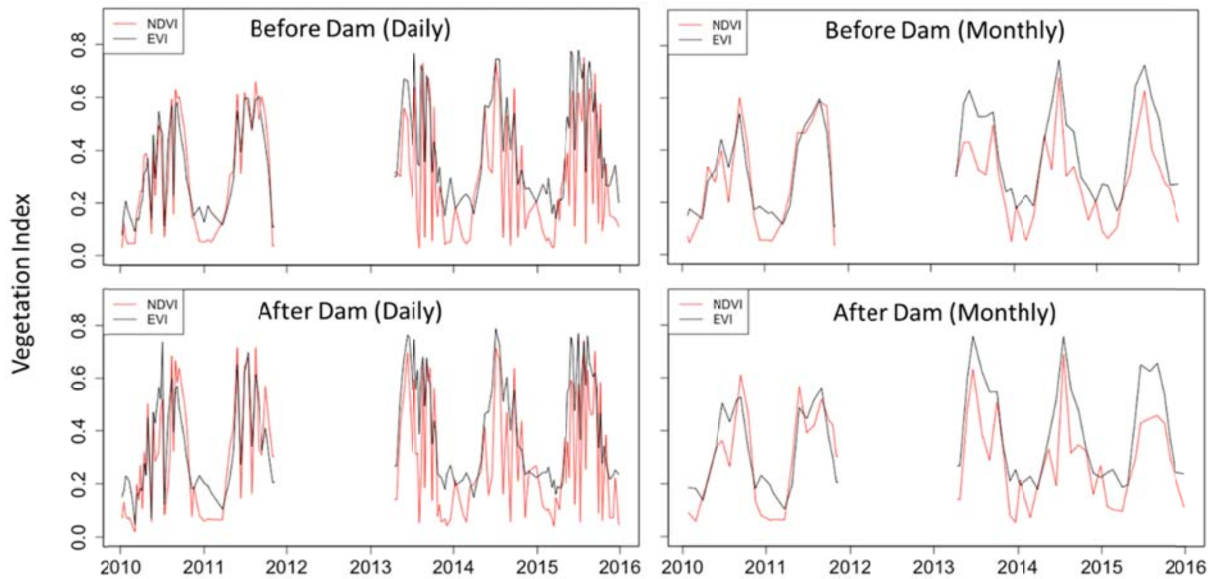

Figure 4. Change in vegetation indices over time

Annual trends within the vegetation index data is very similar across the study period with the expected index peaks during the summer growing season and lows during the winter senescence. However, across the entire study duration, both sections of the river had an overall increase in EVI and NDVI values since 2013. In order to explore this trend and remove the seasonal variation, Figure 5 plots the change in vegetation index values relative to the 2010 image with the closest day or month of the year. As would be expected, both EVI and NDVI have little to no difference in the winter season from 2011 to 2015 compared to the 2010 baseline data; however, there is more significant variation occurring in the summer months. EVI values in general have positive change relative to the 2010 baseline, with peak differences in July and August. NDVI values have both positive and negative differences, with peak deviation from 2010 also occurring in the growing season. Figure 5 shows that the sections of the watershed below and above the dam exhibit similar trends.

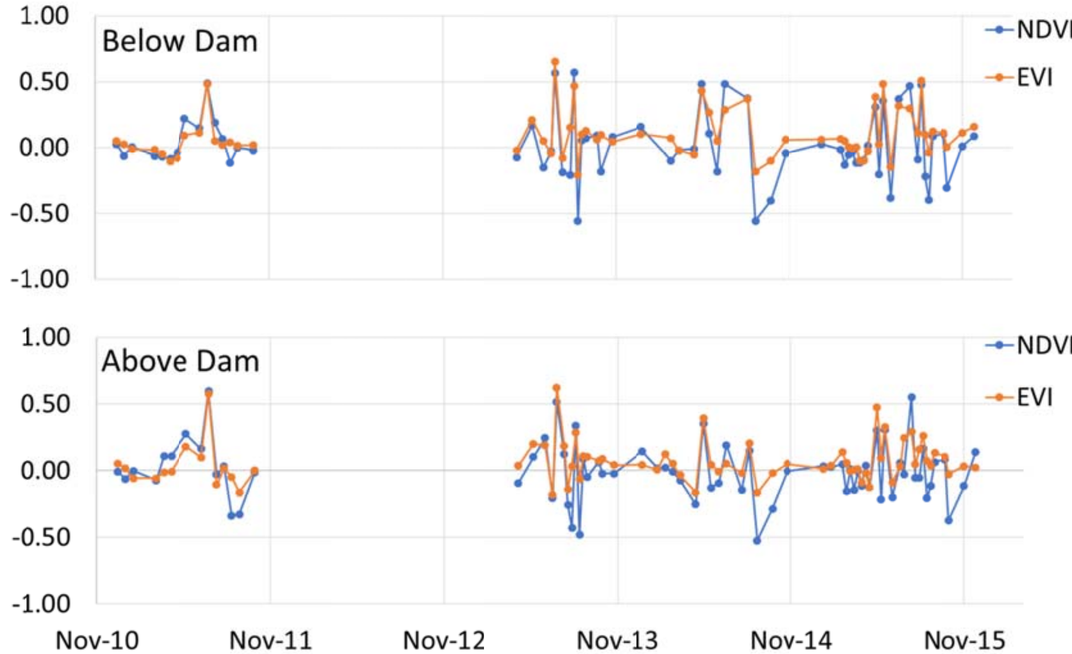

Figure 5. Vegetation Index Value Changes Relative to 2010 Imagery.

Figure 6 and Figure 7 were produced to try to quantify the annual patterns in the changes of EVI and NDVI from 2010 to 2015 based on the 8-day Landsat products. Overall vegetation index data shows that NDVI peaks at 0.7 while EVI peaks at 0.8. As expected, there is a clear increasing trend in both index values from March to May, followed by a period of high index values and then a clear decreasing period from September to November, with the lowest annual index values from December. However, there are also unexpectedly high deviations during the May to September growing season. Fluctuations of the index values are significantly reduced in EVI comparing to NDVI, especially from May to September. Index values during summer season exhibit variation of up to 0.6 for NDVI and up to 0.2 for EVI, which is unlikely to be related to vegetation change. This large variation in values, particularly in NDVI, makes it is hard to quantify the annual trend of these vegetation indices. An exploration of the input imagery suggests that a portion of this apparent variability in index values is related to the presence of image gaps, clouds, and cloud shadows. In order to more fully utilize the GEE datasets, it appears that it is necessary to address these concerns, e.g. through thresholding inputs bands to eliminate non-vegetated areas from areas being evaluated.

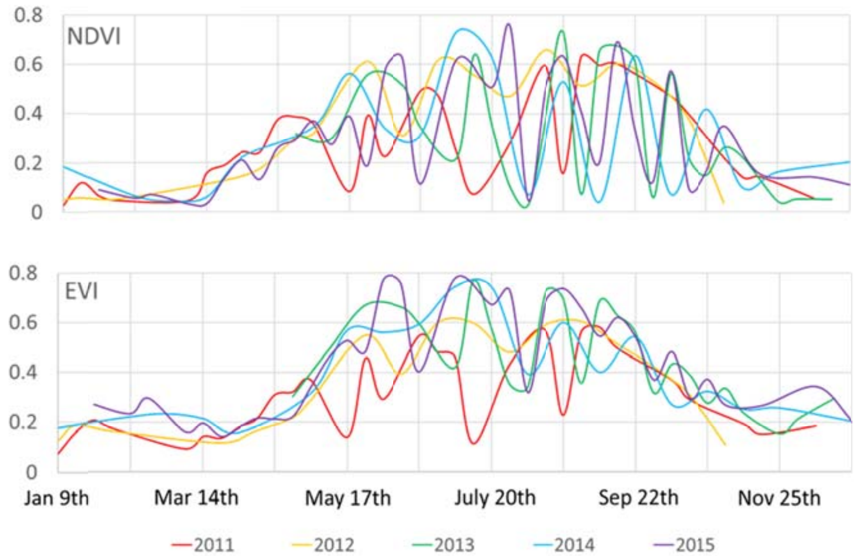

Figure 6. Annual change patterns of vegetation indices (below dam section)

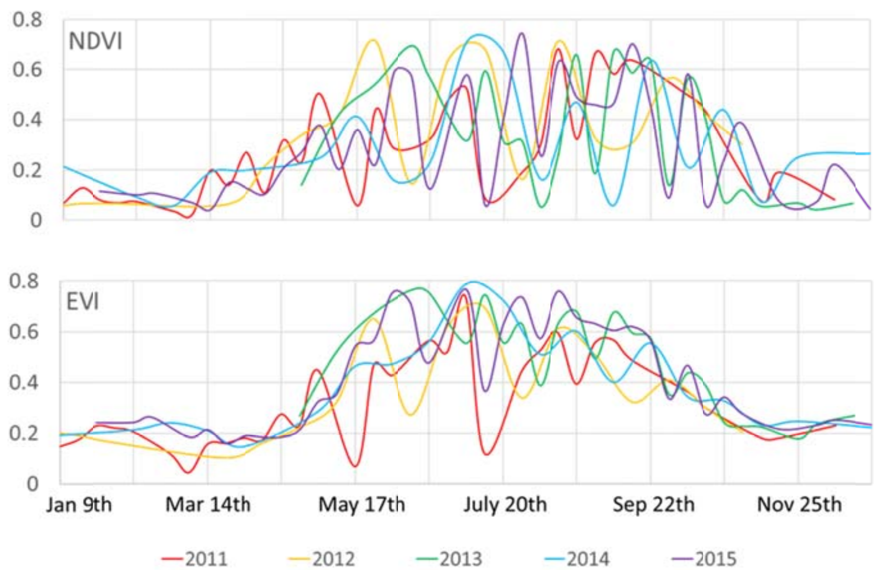

Figure 7. Annual change patterns of vegetation indices (above dam section)

The NDVI and EVI trends illustrate that NDVI appears to be less sensitive to the seasonal variation in vegetation vigor. When the seasonal trend was normalized, there did appear to be an upward trend in the vegetation indices within the riparian zones. However, while the results demonstrated an overall increase in EVI values across the time period, some of this may reflect the differences in sensor configurations onboard Landsat 5 and 8. Next steps of this project should include comparison of the vegetation indices derived from both NAIP and Landsat sensors in order to determine if there needs to be any kind of normalization to utilize these indices when they are derived from the different sensors. Bohon (2014) compared various vegetation index values derived from both Landsat 7 and NAIP imagery, and concluded that the results from the lower spatial resolution imagery did not provide sufficient detail compared to the higher resolution output. Potential future work could utilize the same methodology to compare among NAIP, Landsat 5, Landsat 8 and other sensors to quantify the degree of uncertainties in Landsat driven vegetation indices values for accuracy improvement.

Similarity between the index values before and after the dam suggest that despite the different treatment of the channel, i.e. natural vs. somewhat channelized, there does not appear to be a difference in terms of the riparian vegetation index. Future study should explore the influence of adjacent land uses on the vegetation index values of riparian vegetation, since some land uses (e.g. agricultural or urban) may have greater stress on the riparian zone than others e.g. (forested regions). Wasser et al. (2015) has previously suggested through lidar assessment that riparian forest vegetation structures are strongly associated with adjacent land use.

Correlation

Correlation results were initially explored using the averaged vegetation index values for the watershed for all available Landsat image dates. The correlation coefficients revealed that downstream water temperature and dissolved oxygen have moderate to strong correlation to riparian vegetation index (magnitude of Spearman's correlation coefficient generally above 0.5), while other water quality parameters do not. Water temperature was positively correlated with the vegetation index values, while dissolved oxygen was negatively correlated. In general, EVI values have much higher correlation to the water quality parameters than did NDVI. There were no significant differences in terms of correlation between the two sections of the river (Table 4).

Table 4. Correlation between water quality parameters and vegetation indices. Cells in green highlight where the magnitude of Spearman's correlation coefficient is greater than 0.5.

		Mean Daily Water Quality Parameters				
		Water Temperature	**Specific Conductivity**	**pH**	**Turbidity**	**Dissolved Oxygen**
Above Dam	**NDVI**	0.53	-0.11	-0.20	0.26	-0.53
	EVI	0.79	0.12	-0.24	-0.02	-0.71
Below Dam	**NDVI**	0.56	-0.13	-0.10	0.19	-0.51
	EVI	0.80	0.14	-0.19	-0.13	-0.70

		Minimum Daily Water Quality Parameters				
		Water Temperature	**Specific Conductivity**	**pH**	**Turbidity**	**Dissolved Oxygen**
Above Dam	**NDVI**	0.46	-0.14	-0.26	0.21	-0.46
	EVI	0.79	0.12	0.30	-0.06	-0.74
Below Dam	**NDVI**	0.56	-0.02	-0.19	0.10	-0.54
	EVI	0.83	0.15	-0.27	-0.10	-0.77

		Maximum Daily Water Quality Parameters				
		Water Temperature	**Specific Conductivity**	**pH**	**Turbidity**	**Dissolved Oxygen**
Above Dam	**NDVI**	0.46	-0.10	-0.08	0.24	-0.42
	EVI	0.79	0.16	0.02	0.05	-0.56
Below Dam	**NDVI**	0.55	0.00	0.03	0.16	-0.41
	EVI	0.83	0.18	0.08	0.06	-0.56

When evaluating the correlation between weather data and water quality data, the most significant relationship is between air temperature and water temperature, which is expected (Table 5), although there is also a strong negative relationship between air temperature and dissolved oxygen. Exploring the correlation between vegetation indices and weather data reveals that daily mean air temperature has moderate correlation with vegetation index, which is also to be anticipated since the index values rise during the growing season when the weather is warmer.

Table 5. Correlation results between water quality parameters and weather parameters. Cells in green highlight where the magnitude of Spearman's correlation coefficient is greater than 0.5.

Mean Daily Water Quality Parameters					
	Water Temperature	**Specific Conductivity**	**pH**	**Turbidity**	**Dissolved Oxygen**
Mean Air Temperature	0.93	0.22	-0.13	-0.03	-0.77
Mean Precipitation	0.01	0.00	-0.09	0.08	-0.09

Minimum Daily Water Quality Parameters					
	Water Temperature	**Specific Conductivity**	**pH**	**Turbidity**	**Dissolved Oxygen**
Mean Air Temperature	0.92	0.23	-0.32	-0.17	-0.82
Mean Precipitation	0.00	-0.01	-0.05	0.06	-0.06

Maximum Daily Water Quality Parameters					
	Water Temperature	**Specific Conductivity**	**pH**	**Turbidity**	**Dissolved Oxygen**
Mean Air Temperature	0.92	0.25	0.19	0.06	-0.64
Mean Precipitation	0.00	0.03	-0.09	0.08	-0.12

Many researchers have utilized vegetation indices as a direct measure of vegetation vigor or density. However, the approach to correlation analysis explored in this study needs significant revision in order to remove the effects of seasonal variability, which clearly dominate the results. Without removing this seasonal effect, it is impossible to explore the much more subtle relationship between the vegetation extent within the buffers and water quality.

Channel boundary delineation

This study delineated channel boundaries from NAIP imagery that was acquired at two-year intervals. Redefining the channel was necessary since some areas of the river underwent significant change between image dates (Figure 8). Some of these changes are significant enough to cause the channel to take a different path entirely. Channel variations over time also caused the phenomenon known as channel incision (Shields et al. 2010), which leads to riparian expansion into the channel. This was observed along parts of the river (Figure 9).

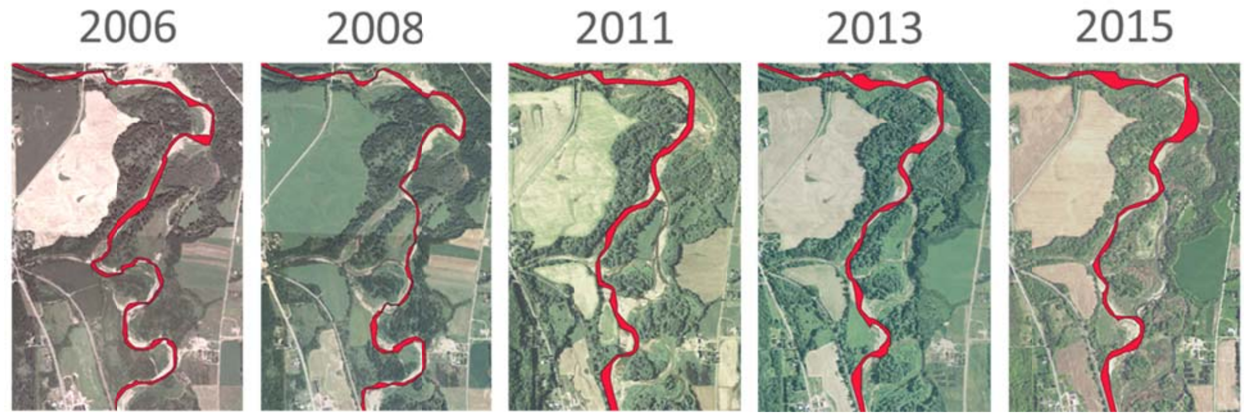

Figure 8. Example Channel Changes Over Time At One Location Along Main Stem of Genesee River

Figure 9. Example Channel Incision and Vegetation Regeneration Along Main Stem of Genesee River

Many studies (e.g., Chase et al. 2016; Fu and Burgher 2015; Weller and Baker 2014; Jones et al. 2010) that have investigated changes in riparian buffers do not incorporate changes within the channel in their analysis. This topic may be a subject for investigation in future projects through comparing long term trends in channels boundary variations and how this impacts—positively and negatively—riparian vegetation extents.

Buffer width

This study utilized a 90m fixed riparian buffer width based on the recommendations of prior studies (Sweeney and Newbold 2014; Hansen et al. 2010; Wenger 1999; Lee, Smyth, and Boutin 2004; Mayer, Reynolds, and Canfield 2005). However, the impact of the riparian buffer width varies depending on factors such as the size of the stream channel and the surrounding land cover (Sweeney and Newbold 2014). Thus it would be valuable to examine the variation in the results of this study under changes in the buffer width. This may be helpful in terms of restoration projects by suggesting optimal riparian buffer width, or locations that could particularly value from vegetation expansion, for different sections of the Genesee River.

Conclusions

Overall, this study developed a new method to rapidly extract time series of riparian vegetation indices directly from satellite image composites. This method was applied to the Genesee River watershed in western New York State and northwestern Pennsylvania. We identified the main channel of the Genesee River and delineated riparian vegetation within 90 meters of the channel for 2011, 2013, and 2015 NAIP imagery, and then characterized the vegetation index within the buffers using Landsat 8-day NDVI and EVI products available through GEE. This project utilized the produced boundaries to investigate the vegetation index within the buffer zone and while observing the expected annual trends, where the index rises in the summer season while falling in the winter season, the analysis also showed that there was a general upward trend in the vegetation values across the study period. Future study should focus on extending the duration of the study to give a much clear picture of how the riparian vegetation perform in the study area, as well as some of the observed short-term channel induced riparian vegetation expansions.

Utilization of GEE in this project brought significant time saving when utilizing vegetation index datasets to analyze riparian vegetation vigor. This project used 300 Landsat scenes covering over five years, which were available preprocessed with derivative products generated. Because of the convenience offered by GEE, the majority of the time and effort was spent on delineating the river channel instead of selecting imagery and deriving NDVI and EVI values. Within a short period, this project was able to delineate the riparian vegetation extent and derive both vegetation index time series values. There does appear to be some issues with cloud cover and gaps that require additional consideration; however, the framework established will allow for such analysis with relatively minor modification.

In this project, biannual riparian vegetation extent data was produced at very high ground resolution at 1m, and the 30 meter vegetation index data was generated on a very high temporal resolution of 8-days. While many studies have reported the value of high spatial detail in managing riparian vegetation, to our knowledge no prior studies have simultaneously explored these resolutions within this context. Higher resolution data from this study will bring many benefits to downstream users, such as easy interpolation and identification of areas which need riparian restoration. Also, stakeholders can now be able to prioritize restoration sites based on both spatial scales and temporal scales.

All vegetation extent and riparian vegetation index data were developed into an online web app and will be shared though a web portal. This pilot study has the potential for easy expansion to other potential riparian vegetation study sites with minimum modification. A detailed step-by-step guide of the processes involved in this study will also be made available through the web portal. Also, included on the web portal is the NDVI and EVI explorer developed using GEE. This tool will give everyone the ability to utilize the convenience of rapid vegetation index extractions from Landsat 5, 7, and 8 imagery.

References

Bohon, R. K. 2014. "Comparing Landsat7 Etm+ and Naip Imagery for Precision Agriculture Application in Small Scale Farming: A Case Study in the South Eastern Part of Pittsylvania County, Va."

Brinson, M. M., L. J. MacDonnell, D. J. Austen, Robert L. Beschta, Theo A. Dillaha, Debra L. Donahue, Stanley V. Gregory, et al. 2002. *Riparian Areas: Functions and Strategies for Management*. *National Academy of Science*. doi:10.17226/661.

Chase, J. W., G. A. Benoy, S. W. R. Hann, and J. M. Culp. 2016. "Small Differences in Riparian Vegetation Significantly Reduce Land Use Impacts on Stream Flow and Water Quality in Small Agricultural Watersheds." *Journal of Soil and Water Conservation* 71 (3). Soil and Water Conservation Society: 194–205.

Fu, B., and I. Burgher. 2015. "Riparian Vegetation NDVI Dynamics and Its Relationship with Climate, Surface Water and Groundwater." *Journal of Arid Environments* 113: 59–68. doi:10.1016/j.jaridenv.2014.09.010.

Hansen, B., P. Reich, S. P. Lake, and T. Cavagnaro. 2010. "Minimum Width Requirements for Riparian Zones to Protect Flowing Waters and Concerne Biodiversity: A Review and Recommendations. With Application to the State of Victoria," no. April: 151. http://www.ccmaknowledgebase.vic.gov.au/resources/RiparianBuffers_Report_Hansenetal2010.pdf.

Huete, A., K. Didan, T. Miura, E. P. Rodriguez, X. Gao, and L. G. Ferreira. 2002. "Overview of the Radiometric and Biophysical Performance of the MODIS Vegetation Indices." *Remote Sensing of Environment* 83 (1–2): 195–213. doi:10.1016/S0034-4257(02)00096-2.

Jones, K., E. Slonecker, S. Nash, C. Neale, G. Wade, and S. Hamann. 2010. "Riparian Habitat Changes across the Continental United States (1972-2003) and Potential Implications for Sustaining Ecosystem Services." *Landscape Ecology* 25 (8): 1261–75. doi:10.1007/s10980-010-9510-1.

Lee, P., C. Smyth, and S. Boutin. 2004. "Quantitative Review of Riparian Buffer Width Guidelines from Canada and the United States." *Journal of Environmental Management* 70 (2): 165–80. doi:10.1016/j.jenvman.2003.11.009.

Makarewicz, J. C., T. W. Lewis, E. Rea, M. J. Winslow, and D. Pettenski. 2015. "Using SWAT to Determine Reference Nutrient Conditions for Small and Large Streams." *Journal of Great Lakes Research* 41 (1). International Association for Great Lakes Research.: 123–35. doi:10.1016/j.jglr.2014.12.022.

Mayer, P. M., S. K. Reynolds, and T. J. Canfield. 2005. "Riparian Buffer Width, Vegetative Cover, and Nitrogen Removal Effectiveness: A Review of Current Science and Regulations." *EPA/600/R-05/118*.

NYS DEC. 2015. "Genesee River Basin Nine Element Watershed Plan for Phosphorus and Sediment."

NYSDEC. 2014. "2014 Section 303 (D) List of Impaired Waters Requiring a TMDL / Other Strategy."

NYSDEC Great Lakes Watershed Program. 2014. "NEW YORK'S GREAT LAKES BASIN: Interim ACTION AGENDA."

Pal, M. 2005. "Random Forest Classifier for Remote Sensing Classification." *International Journal of Remote Sensing* 26 (1): 217–22. doi:10.1080/01431160412331269698.

Patel, N. N., E. Angiuli, P. Gamba, A. Gaughan, G. Lisini, F. R Stevens, A. J Tatem, and G. Trianni. 2014. "International Journal of Applied Earth Observation and Geoinformation

Multitemporal Settlement and Population Mapping from Landsat Using Google Earth Engine." *International Journal of Applied Earth Observations and Geoinformation* 35: 199–208. doi:10.1016/j.jag.2014.09.005.

QGIS Development Team. 2016. "QGIS Geographic Information System." Open Source Geospatial Foundation Project. http://www.qgis.org/.

Salo, J. A., and D. M. Theobald. 2016. "A Multi-Scale, Hierarchical Model to Map Riparian Zones." *River Research and Applications* 22 (July 2011): 1085–95. doi:10.1002/rra.

Shields, F. D., R. E. Lizotte, S. S. Knight, C. M. Cooper, and D. Wilcox. 2010. "The Stream Channel Incision Syndrome and Water Quality." *Ecological Engineering* 36 (1): 78–90. doi:10.1016/j.ecoleng.2009.09.014.

Sweeney, B.W., and J. D. Newbold. 2014. "Streamside Forest Buffer Width Needed to Protect Stream Water Quality, Habitat, and Organisms: A Literature Review." *Journal of the American Water Resources Association* 50 (3): 560–84. doi:10.1111/jawr.12203.

USGS. 2016. "Product Guide." *Product Guide Provisional Landsat 8 Surface Reflectance Code (LaSRC) Product*. doi:10.1080/1073161X.1994.10467258.

Wasser, Leah, Laura Chasmer, Rick Day, and Alan Taylor. 2015. "Quantifying Land Use Effects on Forested Riparian Buffer Vegetation Structure Using LiDAR Data." *Ecosphere* 6 (January): 1–17. doi:10.1890/ES14-00204.1.

Weller, D. E., and M. E. Baker. 2014. "Cropland Riparian Buffers throughout Chesapeake Bay Watershed: Spatial Patterns and Effects on Nitrate Loads Delivered to Streams." *Journal of the American Water Resources Association* 50 (3): 696–712. doi:10.1111/jawr.12207.

Wenger, S. 1999. *A Review of the Scientific Literature on Riparian Buffer Width , Extent and Vegetation*.